



An automated meal detector and bolus calculator in combination with closed-loop blood glucose control

Mahmoudi, Zeinab; Boiroux, Dimitri; Cameron, Faye; Poulsen, Niels Kjølstad; Bequette, B. Wayne; Jørgensen, John Bagterp

Published in:
I F A C Workshop Series

Link to article, DOI:
[10.1016/j.ifacol.2018.11.648](https://doi.org/10.1016/j.ifacol.2018.11.648)

Publication date:
2018

Document Version
Publisher's PDF, also known as Version of record

[Link back to DTU Orbit](#)

Citation (APA):
Mahmoudi, Z., Boiroux, D., Cameron, F., Poulsen, N. K., Bequette, B. W., & Jørgensen, J. B. (2018). An automated meal detector and bolus calculator in combination with closed-loop blood glucose control. *I F A C Workshop Series*, 51(27), 168-173. <https://doi.org/10.1016/j.ifacol.2018.11.648>

General rights

Copyright and moral rights for the publications made accessible in the public portal are retained by the authors and/or other copyright owners and it is a condition of accessing publications that users recognise and abide by the legal requirements associated with these rights.

- Users may download and print one copy of any publication from the public portal for the purpose of private study or research.
- You may not further distribute the material or use it for any profit-making activity or commercial gain
- You may freely distribute the URL identifying the publication in the public portal

If you believe that this document breaches copyright please contact us providing details, and we will remove access to the work immediately and investigate your claim.

An automated meal detector and bolus calculator in combination with closed-loop blood glucose control[★]

Zeinab Mahmoudi^{*} Dimitri Boiroux^{*} Faye Cameron^{**}
 Niels Kjølstad Poulsen,^{*} B. Wayne Bequette^{**}
 John Bagterp Jørgensen^{*}

^{*} *Department of Applied Mathematics and Computer Science,
 Technical University of Denmark, 2800 Kgs. Lyngby, Denmark
 (e-mail: jbj@dtu.dk).*

^{**} *Department of Chemical and Biological Engineering, Rensselaer
 Polytechnic Institute, Troy, NY, USA (e-mail: bequette@rpi.edu).*

Abstract: The aim of this study is to develop an algorithm for detection of unannounced meals and an insulin bolus calculator (BC) to work in combination with the meal detector. The input of the meal detector are the continuous glucose monitoring (CGM) data and the insulin infusion rate. During daytime, the automated meal detector and the BC control the blood glucose concentration. During nighttime, a model predictive control (MPC) algorithm regulates the basal insulin rate. The meal detector detects the occurrence of a meal, estimates the amount of carbohydrate (CHO) in the meal, and estimates the meal onset time. The BC computes a bolus dose to cover the detected meal. We test the meal detector and the BC on nine virtual type 1 diabetes (T1D) patients. The meal detection algorithm, applied on the virtual patients, has a median detection delay of 40 min, detection sensitivity of 80% and a median meal onset estimation bias of 15 min. The algorithm does not have false positive.

© 2018, IFAC (International Federation of Automatic Control) Hosting by Elsevier Ltd. All rights reserved.

Keywords: Type 1 diabetes, Meal detection, Kalman filter, Bolus calculator.

1. INTRODUCTION

It is crucial that people with type 1 diabetes (T1D) receive adequate and prompt meal bolus insulin to lower postprandial blood glucose (BG) and to achieve the target hemoglobin A1C (HbA1C) level (Burdick et al., 2004). Prandial BG control is a challenge for open-loop basal-bolus insulin therapy and for artificial pancreas (AP) systems. Several AP studies challenge their AP by unannounced meals without meal announcement or meal detection techniques (Dassau et al., 2017; Chakrabarty et al., 2017; Pinsky et al., 2016; Reddy et al., 2016). A traditional approach to overcome the challenge of postprandial BG control is prandial announcement or manual bolus administration (Emami et al., 2017; Breton et al., 2012; Phillip et al., 2013). Nevertheless, these actions require patient's intervention which increases the safety risks due to the nonadherence of the patient to meal announcements (Bequette, 2012; Cameron et al., 2014, 2012). Automated meal detection and meal-size estimation is another approach to cope with meal challenge, and it can be a safety feature for patients who frequently forget to enter meal information to their therapeutic device.

The aim of the current study is to develop an algorithm for detection of unannounced meals which can be used in an AP or in an open-loop basal-bolus insulin therapy. We

use the meal detection algorithm in the latter case and we limit the closed-loop BG control to nighttime when the patient does not take a meal. We also develop a user friendly model identification method for the meal detector. The identification method is easy to use in the clinical setups. For postprandial BG control, we develop an insulin bolus calculator (BC) that works in combination with the meal detector. We demonstrate that combining the meal detector with the bolus calculator can reduce the postprandial glycemic variability.

The rest of the paper is organized as follows. Section 2 describes the methods of the study. After giving a brief summary of the meal detection algorithm, we present the input-output model and the converted state-space model for the meal detector. Then we explain the model identification method. Later in this section, we explain the different parts of the meal detector and we continue with introducing the BC. The next subsection of Section 2 describes the model predictive control (MPC) for the nighttime BG regulation. Section 3 presents the results and discussion. Section 4 contains the conclusion of the paper.

2. MATERIALS AND METHODS

2.1 The meal detection algorithm: a brief summary

We use the Medtronic Virtual Patient (MVP) as the T1D simulator (Kanderian et al., 2009). The MVP model con-

[★] This work is funded by the Danish Diabetes Academy supported by the Novo Nordisk Foundation, NIH grant number 1R01DK102188, NSF grant.

tains the pharmacokinetics and pharmacodynamics of insulin and BG, and the two-compartmental model of CHO absorption by Hovorka et al. (2008). u_I is the subcutaneous (SC) insulin input rate (U/min) and contains both basal and bolus insulin administrations. The continuous glucose monitoring (CGM) is corrupted by measurement noise, v . The unannounced meal disturbance u_{d1} denotes the CHO ingestion rate (g/min). A Kalman filter (KF) estimates u_{d1} along with other states of the model. The model in the KF is based on a linear input-output relation between BG and insulin and between BG and CHO. The innovation of the KF enters a cumulative sum (CUSUM) change detection algorithm. The CUSUM algorithm applies a statistical test on the innovation and announces the occurrence of a change if the alternative hypothesis of the test is accepted. When the CUSUM test detects a change in the innovation and \hat{u}_{d1} exceeds a data-derived threshold, a Rauch-Tung-Striebel (RTS) fixed-interval smoother estimates $\hat{u}_{d1,k|k_a}$, for $k = \hat{k}_s, \dots, k_a - 1$. The time instant, k_a , is the detection time and \hat{k}_s is the estimated meal onset. An integrator calculates the meal-size by integrating the smoothed estimates, $\hat{u}_{d1,k|k_a}$. If the estimated meal size is greater than a pre-defined threshold, the meal detector announces the presence of a meal and the BC computes an insulin bolus for the detected meal.

2.2 The input-output model

The input-output model for insulin and food intake is a second order linear model. In the Laplace domain it is defined as:

$$Y(s) = \frac{K_I}{(\tau_I s + 1)^2} U_I(s) + \frac{K_d}{(\tau_d s + 1)^2} U_{d1}(s). \quad (1)$$

The output $Y(s)$ is the change in the BG concentration in Laplace domain. $U_I(s)$ is the SC insulin input rate (U/min), and $U_{d1}(s)$ is the rate of ingested CHO (g/min). The gains, K_I and K_d , correspond to the steady state change in BG, and the time constants, τ_I and τ_d , determine the time it takes to reach the steady state.

2.3 The state-space model

A canonical realization of the model in (1) provides the state-space matrices A , B_I , B_d , and C . These matrices depend on the estimates of the unknown parameter vector, $\theta = [K_I \ K_d \ \tau_I \ \tau_d]^T$. An integrated white noise models the ingested meal. Therefore, the meal disturbance adds two states to the model which are u_{d1} and u_{d2} . The state-space model in the stochastic differential equation (SDE) form is

$$dx(t) = \left(A(\theta)x(t) + B_I(\theta)u_I(t) + B_d(\theta)u_{d1}(t) \right) dt + G_x d\omega(t), \quad (2a)$$

$$du_{d1}(t) = u_{d2}(t)dt, \quad (2b)$$

$$du_{d2}(t) = Gd\omega(t), \quad d\omega(t) \sim N(0, Idt), \quad (2c)$$

$$y_k = C(\theta)x_k + v_k, \quad v_k \sim N(0, R), \quad (2d)$$

$$G_x = [\sigma_{x1} \ \sigma_{x2} \ \sigma_{x3} \ \sigma_{x4}]^T. \quad (2e)$$

The input, u_{d1} , is the ingested CHO rate (g/min), and u_{d2} (g/min²) is the rate of change of u_{d1} . The process noise, $d\omega$, is a standard Wiener process and v is the sensor noise. The output, y , is the CGM measurement. As u_{d1} and u_{d2}

are unknown, the original states, x , are augmented with the CHO state vector, $u_d^a = \begin{bmatrix} u_{d1} \\ u_{d2} \end{bmatrix}$, for estimation by the KF. The augmented state-space model is

$$dx^a(t)dt = \left(A^a(\theta)x^a(t) + B^a(\theta)u_I(t) \right) dt + G^a d\omega(t), \quad (3a)$$

$$d\omega(t) \sim N(0, Idt), \quad (3b)$$

$$y_k = C^a(\theta)x_k^a + v_k \quad v_k \sim N_{iid}(0, R), \quad (3c)$$

where $x^a(t) = \begin{bmatrix} x(t) \\ u_d^a(t) \end{bmatrix}$. Combining matrices A , B_I , B_d , C ,

G , and G_x with blocks of zero matrices (with appropriate dimension) gives the augmented matrices A^a , B^a , C^a , and G^a . The continuous-discrete-time stochastic linear state space model in (3) is converted to the discrete-time stochastic linear model

$$x_{k+1}^a = A^{a,d}x_k^a + B^{a,d}u_{I,k} + w_k, \quad (4a)$$

$$z_k = C^a x_k^a, \quad (4b)$$

$$y_k = z_k + v_k \quad (4c)$$

$$w_k \sim N_{iid}(0, Q), \quad (4d)$$

$$v_k \sim N_{iid}(0, R). \quad (4e)$$

A discrete KF estimates the augmented state vector, x^a .

2.4 The discrete-time KF for meal estimation

The discrete KF estimates the augmented states, $x_{k|k}^a$, and their covariance, $P_{k|k}$ (Mahmoudi et al., 2017, 2016). The one-step prediction for the mean and covariance is

$$\hat{x}_{k|k-1}^a = A^{a,d}\hat{x}_{k-1|k-1}^a + B^{a,d}u_{I,k-1}, \quad (5a)$$

$$P_{k|k-1} = A^{a,d}P_{k-1|k-1}[A^{a,d}]^T + Q. \quad (5b)$$

The corresponding one-step ahead prediction of the measurement, $\hat{y}_{k|k-1}$, is given by

$$\hat{y}_{k|k-1} = \hat{z}_{k|k-1} = C^a \hat{x}_{k|k-1}^a, \quad (6)$$

such that the innovation, e_k , and its covariance, R_{e_k} , can be computed as

$$e_k = y_k - \hat{y}_{k|k-1}, \quad (7a)$$

$$R_{e,k} = C^a P_{k|k-1} [C^a]^T + R, \quad (7b)$$

in which $R = \sigma_v^2$. The KF gain is

$$K_k = P_{k|k-1} [C^a]^T R_{e,k}^{-1} \quad (8)$$

and the filtered mean, $\hat{x}_{k|k}^a$, and covariance, $P_{k|k}$, for the augmented states are

$$\hat{x}_{k|k}^a = \hat{x}_{k|k-1}^a + K_k e_k, \quad (9a)$$

$$P_{k|k} = P_{k|k-1} - K_k R_{e,k} K_k^T. \quad (9b)$$

The filtered augmented state vector is

$$\hat{x}_{k|k}^a = [\hat{x}_{k|k}; \hat{u}_{d1,k|k}; \hat{u}_{d2,k|k}].$$

2.5 Model identification

Insulin transfer function We use the impulse response identification method to estimate the parameter, $\theta = [K_I \ K_d \ \tau_I \ \tau_d]^T$. The unit insulin impulse response is

$$h_I(t) = K_I(t/\tau_I^2) \exp(-t/\tau_I). \quad (10)$$

The time constant, τ_I , is equivalent to the insulin action time. Using the insulin impulse response, we identify τ_I ,

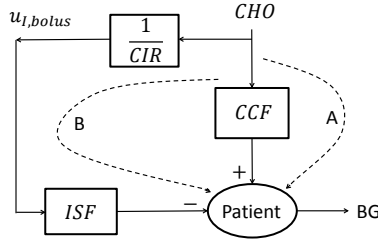


Fig. 1. A simple model that describes the routes where meal and insulin exert their effects on the BG concentration. CCF is the CHO conversion factor, CIR is CHO to insulin ratio and ISF is the insulin sensitivity factor.

K_I , and the insulin sensitivity factor, ISF (mg/dL/IU) following the method by Boiroux et al. (Boiroux et al., 2017a). In practice, the patients and their caregivers empirically determine ISF and τ_I for daily insulin dose adjustments. By knowing τ_I and ISF and using the insulin impulse response, the gain, K_I is identified as

$$K_I = \tau_I \exp(1) ISF. \quad (11)$$

CHO transfer function For identification of the gain, K_d , and the time constant, τ_d , we do the following procedure. The simple model in Fig. 1 demonstrates the routes with which insulin and meal exert their effect on BG. In route A, the CHO conversion factor, CCF (mg/dL/g), converts the CHO in u_{d1} into a corresponding increase in BG. In route B, the ISF converts u_I into a corresponding reduction in BG. The CHO-to-insulin-ratio, CIR (g/IU) is an estimate of the grams of CHO that one unit of rapid-acting insulin can cover. Caregivers and patients use the 500 Rule for CIR calculation, $CIR = 500/TDD$, where TDD is the total daily dose of insulin. The TDD of the MVP patients is given in the study by Kanderian et al. (2009). We also use the 500 Rule in the study. The bolus insulin dose, $u_{I,bolus}$, computed according to $u_{I,bolus} = CHO/CIR$, covers the CHO content in u_{d1} (Boiroux et al., 2017b). Ideally, the maximum reduction in the BG due to $u_{I,bolus}$ should compensate the maximum increase in BG caused by the CHO in u_{d1} . This is equivalent to $u_{I,bolus} \cdot ISF = CHO \cdot CCF$. Therefore an estimate of CCF is given as $CCF = ISF/CIR$.

The unit CHO impulse response is

$$h_d(t) = K_d(t/\tau_d^2) \exp(-t/\tau_d). \quad (12)$$

The CHO impulse response has its peak at τ_d ,

$$y_{d,max} = CHO \cdot h_{d,max} = CHO \cdot K_d(1/\tau_d) \exp(-1). \quad (13)$$

CCF causes the peak in y_d , and the relation between the peak and the CCF is described as

$$y_{d,max} = CHO \cdot CCF. \quad (14)$$

Using (13) and (14), an expression for K_d is given by

$$K_d = \tau_d \exp(1) CCF. \quad (15)$$

The solution to the least squares optimization problem below gives an estimate of K_d and τ_d :

$$\min_{\tau_d, K_d} \phi(\tau_d, K_d) = \frac{1}{2} \sum_{i=1}^{N_y} \|y(t_i) - \hat{y}(t_i, \tau_d, K_d)\|_2^2, \quad (16a)$$

s.t.

$$30 \leq \tau_d \leq 300, \quad (16b)$$

$$K_d = \tau_d \exp(1) CCF, \quad (16c)$$

$$x(t=0) = x_0(=0), \quad (16d)$$

$$u(t=0) = u_0(=0), \quad (16e)$$

$$\dot{x} = A(\tau_d, K_d)x(t) + B(\tau_d, K_d)u(t) \quad (16f)$$

$$\hat{y} = C(\tau_d, K_d)x(t). \quad (16g)$$

The matrix B is $[B_I, B_d]$, and the input, u , contains insulin and meal, i.e., $u = [u_I, u_{d1}]^T$. The output y is the CGM data. The patient ingests the meal, u_{d1} , with a known CHO content and takes the bolus insulin, $u_{I,bolus}$, to cover the meal.

2.6 The CUSUM algorithm for meal detection

A CUSUM test detects the ingestion of a meal and estimates the onset time by applying a statistical test on the sequence of random variable $\{z_i\}_{i=1,2,\dots}$, where $z_i = e_i$ and e is the KF innovation. The variable z has the mean μ and variance σ^2 . The problem is to detect whether μ is large enough to be detected as a meal, and what is the onset of meal-related change in μ . The change detection problem is then:

- to detect whether a meal is ingested,
- to estimate the meal start time, t_s ,

The hypotheses of the change detection in the innovation are:

$$\begin{aligned} \mathcal{H}_0 : \mu &= \mu_0 \quad \text{for } 1 \leq i \leq k, \\ \mathcal{H}_1 : \mu &= \mu_0 \quad \text{for } 1 \leq i \leq k_0 - 1 \quad \text{and} \\ &\mu = \mu_1 \quad \text{for } k_0 \leq i \leq k, \end{aligned} \quad (17)$$

where the time instant k_0 is unknown. μ_0 is the mean of $\{z_i\}_{i=1,2,\dots}$ when no meal is ingested, and μ_1 is the mean of z when the variable z is under the effect of meal. The time sample k_0 is the onset of change in z . The CUSUM test detects a change whenever it accepts \mathcal{H}_1 . For testing the hypotheses, we use the recursive form of the CUSUM decision function defined as

$$g(k) = \max \left(0, g(k-1) + e_k - \mu_0 - \frac{\beta}{2} \right). \quad (18)$$

The CUSUM change detection test is:

$$\begin{aligned} \text{If } g(k) &\leq \bar{h} \quad \text{accept } \mathcal{H}_0, \\ \text{If } g(k) &> \bar{h} \quad \text{accept } \mathcal{H}_1. \end{aligned} \quad (19)$$

The threshold \bar{h} is defined as $\bar{h} = h\hat{\sigma}^2/\beta$, where $\hat{\sigma}$ is the empirical estimates of σ (Blanke et al., 2006). β is twice the absolute change magnitude from μ_0 to μ_1 that one wishes to detect as a meal. h is a positive threshold which is a tuning parameter of the CUSUM algorithm. Blanke et al. (Blanke et al., 2006) describes a method for the optimal tuning of h for the CUSUM test. The initial value of g is set to $g(-1) = 0$.

Estimating the meal onset time The CUSUM algorithm can estimate the time, t_0 , which is the onset of change in the KF innovation. The time instant, k_0 , corresponds to t_0 in discrete time, i.e., $t_0 = k_0\Delta t$, where Δt is the

sensor sampling time. If \mathcal{H}_1 is accepted, the CUSUM algorithm gives an estimate of k_0 as $\hat{k}_0 = k_a - N(k_a)$. The count, N , is the number of successive observations for which the decision function g remains strictly positive and is computed as $N(k) = N(k-1) 1_{\{g(k-1) > 0\}} + 1$. The time that a meal starts to increase CGM approximately coincides with the onset of change in the innovation signal. Therefore, an estimate of k_0 gives an estimate of the onset of the meal-related rise in the CGM signal. The time, k_a , is the instant that the CUSUM algorithm detects the change, i.e., the time for which $g(k)$ crosses the threshold \hat{h} . We assume that the onset of the detected meal is the same as the onset of change in the innovation, and therefore, an estimate of the meal onset time, \hat{k}_s , is

$$\hat{k}_s = \hat{k}_0. \quad (20)$$

2.7 Meal detection and CHO estimation

The algorithm uses two tests to announce a meal, 1) a CUSUM test on e_k and 2) a comparison with a threshold applied on $\hat{u}_{d1,k|k}$. If the CUSUM test accepts \mathcal{H}_1 in (19) at time, k_a , and $\hat{u}_{d1,k_a|k_a} > h_d$, the meal detector goes to the next step. The threshold, h_d , is the maximum of $\hat{u}_{d1,k|k}$ in the tuning interval,

$$h_d = \max\{\hat{u}_{d1,k|k} | k = 1, 2, \dots, k_{tuning}\}. \quad (21)$$

The interval is the same as the tuning interval for the CUSUM test, which is the first 6 hours (nighttime) of the data where the patient does not ingest any meal. If both tests detect a change (the CUSUM test accepts \mathcal{H}_1 and $\hat{u}_{d1,k_a|k_a} > h_d$), then a fixed-interval RTS smoother estimates $\hat{u}_{d1,k|k_a}$ in the interval between the estimated change onset, \hat{k}_s , and the detection instant, k_a . For estimating the amount of CHO in the meal, the algorithm integrates the smoothed estimates, $\hat{u}_{d1,k|k_a}$, as follows.

$$C\hat{H}O = \sum_{k=\hat{k}_s}^{k_a-1} \hat{u}_{d1,k|k_a} \Delta t. \quad (22)$$

If $C\hat{H}O > 20$ g, the algorithm announces a meal and it saves $C\hat{H}O$ as the estimated meal-size and saves \hat{k}_s as the estimated meal onset. The meal detector allows detection of a new meal if the time elapsed from the ending of the previously detected meal is at least 2 h.

2.8 Meal insulin bolus calculator (BC)

In order to evaluate the efficacy of the meal detector for BG regulation, we combine it with a BC. We develop a BC which is adapted to the meal detector. The BC works as follows. The algorithm detects a meal and estimates the meal-size at time, t_a , according to (22).

The bolus insulin to be given at time t_a is computed by

$$\hat{u}_{I,bolus}(t_a) = \frac{C\hat{H}O}{CIR} + \alpha \frac{y(t_a) - BG_{target}}{ISF}, \quad (23)$$

where $y(t_a) = y_{k_a}$ is the noisy CGM measurement at time t_a corresponding to sample, k_a . The term, $(C\hat{H}O)/CIR$, covers the meal, while $\alpha(y(t_a) - BG_{target})/ISF$ corrects for the deviation from the target BG level. The coefficient, α , is a tuning parameter. The structure is similar to a normal bolus calculator when the meal is announced (Boiroux

et al., 2017a). The key modification is that (23) accounts for the fact that the meal is detected and estimated some time after it is taken, i.e. $t_a > t_s$.

2.9 Nocturnal BG regulation with MPC

During nighttime (00:00 h - 6:00 h), an MPC adjusts the basal insulin rate. In each time sample, an MPC algorithm solves an open-loop optimal control problem and implements only the control action corresponding to the first sample interval in the closed loop. The optimal control problem solved in each sample interval is

$$\min_{\{\hat{u}_{I,k+j|k}, \hat{v}_{k+j+1|k}\}_{j=0}^{N-1}} \phi, \quad (24a)$$

s.t.

$$\hat{x}_{k+1|k} = A_I \hat{x}_{k|k-1} + B_I \hat{u}_{I,k|k} + K e_k, \quad (24b)$$

$$\hat{x}_{k+1+j|k} = A_I \hat{x}_{k+j|k} + B_I \hat{u}_{I,k+j|k}, \quad j = 1, \dots, N-1, \quad (24c)$$

$$\hat{y}_{k+1+j|k} = C_I \hat{x}_{k+1+j|k} \quad j = 1, \dots, N, \quad (24d)$$

$$u_{I,min} \leq \hat{u}_{I,k+j|k} \leq u_{I,max}, \quad j = 0, \dots, N-1, \quad (24e)$$

where the objective function, ϕ , is defined as

$$\phi = \frac{1}{2} \sum_{j=0}^{N-1} \|\hat{y}_{k+j+1|k} - \hat{r}_{k+j+1|k}\|_2^2 + \frac{1}{2} \sum_{j=0}^{N-1} \lambda \|\Delta \hat{u}_{I,k+j|k}\|_2^2. \quad (25)$$

e is the Kalman filter innovation and K is the filter gain. $u_{I,min} = -u_{I,ss}$, where $u_{I,ss}$ is the steady-state basal insulin rate. The matrices A_I , B_I , and C_I are obtained from the insulin transfer function. $u_{I,max}$ and the BG target trajectory, r , are defined in Boiroux et al. (2017a).

3. RESULTS AND DISCUSSION

We use 9 virtual T1D patients in Kanderian et al. (2009) (patients 1 to 10 excluding patient 2). The simulation time is 36 hours for each patient starting from 12 midnight (0:00 h) of the first day and ending at 12 noon of the next day. The virtual patients take five meals including breakfast (for two days), lunch, dinner, and snack. For all simulations, during nighttime (0:00 h - 6:00 h) an MPC adjusts the basal insulin delivery rate. The MPC is off during daytime and the basal-bolus insulin therapy regulates the BG concentration. For all simulations in the paper, $\alpha = 0.5$ in (23), and the duration of the postbolus basal insulin suspension is two hours.

Fig. 2 shows an example of comparing regular basal-bolus therapy with the modified basal-bolus therapy (suspending basal insulin for two hours after each bolus) when using meal detector for both cases. A meal detector that works based on the CGM signal has an inevitable detection delay. Therefore at meal detection time, which is naturally delayed with respect to the actual meal onset, the BG concentration is already elevated and the CHO in the meal has partially exerted its effect on BG. When the patient takes a bolus insulin at meal detection time, the slow insulin action can cause a late postprandial hypoglycemia. The postbolus suspension of basal insulin that occurs in the modified basal-bolus insulin delivery reduces the risk of the late postprandial hypoglycemia. During daytime, for the intervals that the basal insulin is not suspended, the basal insulin, $u_{I,ss}$, is computed from the steady state

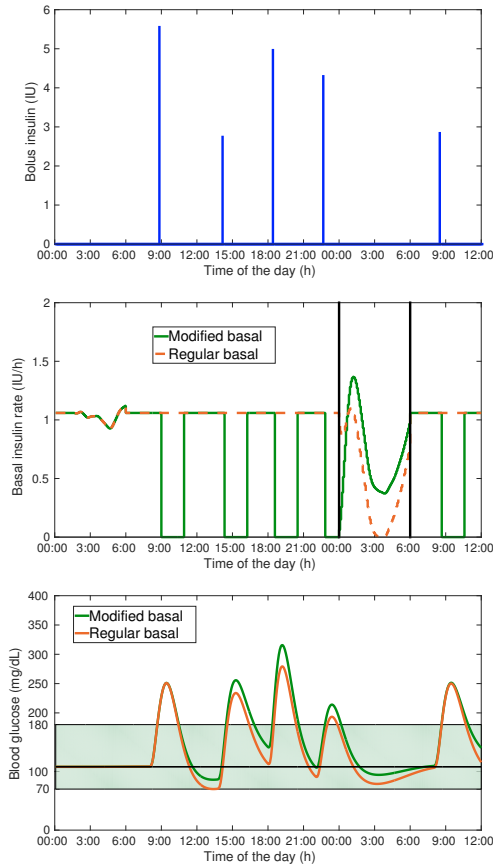


Fig. 2. Example of BG control with modified basal-bolus and the regular basal-bolus methods. For both cases, the meal detector detects the meals and the bolus calculator gives the meal boluses according to the calculated meal size. In the modified basal-bolus method, first a bolus is calculated for each meal and then the basal insulin rate is blocked for two hours after the bolus. The middle plot is the basal insulin rates. An MPC regulates the basal insulin rate during nighttime (00:00 h - 6:00 h).

calculation of the virtual patient. In practise, clinicians determine an optimal basal insulin rate for BG regulation.

Table 1 presents the meal detection results for the patients. t_a is the time at which meal is detected, t_s is the actual meal onset, \hat{t}_s is the estimated meal onset, and \hat{CHO} is the estimated CHO of the meal. Table 2 compares the consensus glycemic outcomes (Maahs et al., 2016; Monnier et al., 2017) in three cases: 1) with meal detector in use, 2) with meal announcement with correct timing and correct CHO size, and 3) without any meal insulin bolus.

Table 1 indicates that in general, the meal detector underestimates the meal size. As Table 2 shows, the meal detector does not increase the percentage of time in hypoglycemia compared to the meal announcement case. This is indicative of safety of the proposed meal detection algorithm.

4. CONCLUSIONS

We developed a meal detection algorithm and a combined bolus calculator for postprandial blood glucose regulation.

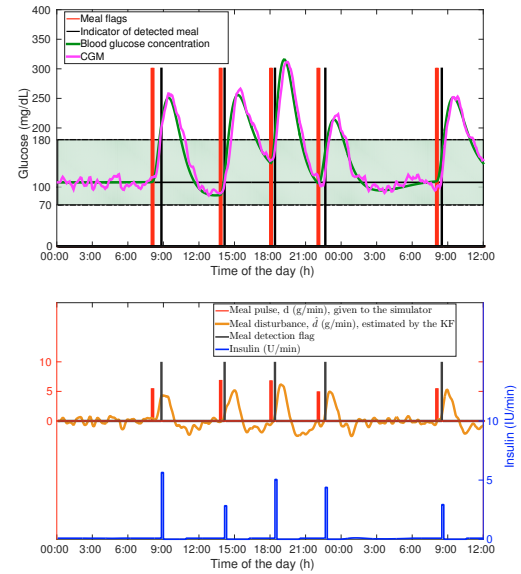


Fig. 3. Example of meal detection for a virtual type 1 diabetes patient.

For the overnight BG control, we used an MPC algorithm that adjusts the rate of basal insulin. The meal detection method is based on a KF and a CUSUM change detector. The meal detector could reduce the mean glucose level without increasing the time in hypoglycemia.

REFERENCES

- Bequette, B.W. (2012). Challenges and recent progress in the development of a closed-loop artificial pancreas. *Annual Reviews in Control*, (2), 255–266.
- Blanke, M., Lunze, J., Kinnaert, M., Staroswiecki, M., and Schröder, J. (2006). *Diagnosis and fault-tolerant control*. Springer Berlin Heidelberg.
- Borroux, D., Duun-Henriksen, A.K., Schmidt, S., Nørgaard, K., Poulsen, N.K., Madsen, H., and Jørgensen, J.B. (2017a). Adaptive control in an artificial pancreas for people with type 1 diabetes. *Control Engineering Practice*, 58, 332–342.
- Borroux, D., Aradóttir, T., Nørgaard, K., Poulsen, N.K., Madsen, H., and Jørgensen, J.B. (2017b). An adaptive nonlinear basal-bolus calculator for patients with type 1 diabetes. *Journal of Diabetes Science and Technology*, 11(1), 29–36.
- Breton, M., Farret, A., Bruttomesso, D., Anderson, S., Magni, L., Patek, S., Man, C., Place, J., Demartini, S., Del Favero, S., Toffanin, C., Hughes-Karvetski, C., Dassau, E., Zisser, H., Doyle, F., De Nicolao, G., Avogaro, A., Cobelli, C., Renard, E., and Kovatchev, B. (2012). Fully integrated artificial pancreas in type 1 diabetes: Modular closed-loop glucose control maintains near normoglycemia. *Diabetes*, 61(9), 2230–2237.
- Burdick, J., Chase, H., Slover, R., Knievel, K., Scrimgeour, L., Maniatis, A., and Klingensmith, G. (2004). Missed insulin meal boluses and elevated hemoglobin a1c levels in children receiving insulin pump therapy. *Pediatrics*, 113(3), e221–224.
- Cameron, F., Niemeyer, G., and Bequette, B.W. (2012). Extended multiple model prediction with application to blood glucose regulation. *Journal of Process Control*, 22(8), 1422–1432.

Table 1. Meal detection performance for 9 virtual T1D patients (13.5 days and 45 meals).

Metrics	Value
Detection delay (min): $t_a - t_s$	40 [35 50]*
Meal onset time estimation bias (min): $ \hat{t}_s - t_s $	15 [5 25]
Number of false positives	0
Number of false negatives	9
Number of underestimated meals	31
CHO estimation bias for underestimated meals(g): $C\hat{H}O - CHO$	-32 [-58 -18]
Number of overestimated meals	4
CHO estimation bias for overestimated meals(g): $C\hat{H}O - CHO$	5 [2 6]

* Median [interquartile range].

Table 2. The consensus glycemic metrics for 9 T1D patients. The three cases are 1) meal detection, 2) meal announcement, and 3) Without meal bolusing.

Glycemic metrics	Detected	Announced	Unbolused meals
Mean CGM glucose (mg/dL)	152.9 (12.6)*	137.5 (16.3)	185.3 (28.5)
% CGM time < 50 mg/dL	0 (0)	0 (0)	0 (0)
% CGM time < 60 mg/dL	0 (0)	0 (0)	0 (0)
% CGM time < 70 mg/dL	0 (0)	0 (0)	0 (0)
% CGM time 70-140 mg/dL	49.1 (12.9)	61.9 (17.2)	37.8 (7.5)
% CGM time 70-180 mg/dL	71.6 (9.4)	85.6 (14.0)	52.0 (11.3)
% CGM time > 180 mg/dL	28.4 (9.4)	14.4 (14.0)	48.0 (11.3)
% CGM time > 250 mg/dL	4.2 (4.5)	0.7 (1.1)	19.8 (14.7)
% CGM time > 300 mg/dL	0.4 (0.8)	0 (0)	8.1 (11.6)

* Mean (SD).

- Cameron, F., Niemeyer, G., Wilson, D.M., Bequette, B.W., Benassi, K.S., Clinton, P., and Buckingham, B.A. (2014). Inpatient trial of an artificial pancreas based on multiple model probabilistic predictive control with repeated large unannounced meals. *Diabetes Technology and Therapeutics*, 16(11), 728–734.
- Chakrabarty, A., Zavitsanou, S., Doyle III, F., and Dassau, E. (2017). Event-triggered model predictive control for embedded artificial pancreas systems. *IEEE Transactions on Bio-medical Engineering*, 1–12.
- Dassau, E., Renard, E., Place, J., Farret, A., Pelletier, M., Lee, J., Huyett, L., Chakrabarty, A., Doyle, F., and Zisser, H. (2017). Intraperitoneal insulin delivery provides superior glycaemic regulation to subcutaneous insulin delivery in model predictive control-based fully-automated artificial pancreas in patients with type 1 diabetes: a pilot study. *Diabetes, Obesity and Metabolism*, 0, 1–8.
- Emami, A., Willinska, M., Thabit, H., Leelarathna, L., Hartnell, S., Dellweg, S., Benesch, C., Mader, J., Holzer, M., Kojzar, H., Pieber, T., Arnolds, S., Evans, M., and Hovorka, R. (2017). Behavioral patterns and associations with glucose control during 12-week randomized free-living clinical trial of day and night hybrid closed-loop insulin delivery in adults with type 1 diabetes. *Diabetes Technology and Therapeutics*, 19(7), 433–437.
- Hovorka, R., Chassin, L.J., Ellmerer, M., Plank, J., and Wilinska, M.E. (2008). A simulation model of glucose regulation in the critically ill. *Physiological Measurement*, 29(8), 959–978.
- Kanderian, S., Weinzimer, S., Voskanyan, G., and Steil, G. (2009). Identification of intraday metabolic profiles during closed-loop glucose control in individuals with type 1 diabetes. *Journal of Diabetes Science and Technology*, 3(5), 1047–1057.
- Maahs, D.M., Buckingham, B.A., and et al. (2016). Outcome measures for artificial pancreas clinical trials: A consensus report. *Diabetes Care*, 39(7), 1175–1179.
- Mahmoudi, Z., Lyngbye, W.S., Boiroux, D., M, H., Nørgaard, K., Poulsen, N.K., Madsen, H., and Jørgensen, J.B. (2016). Comparison of three nonlinear filters for fault detection in continuous glucose monitors. *Ieee Engineering in Medicine and Biology Society Conference Proceedings*, 2016-, 3507–3510.
- Mahmoudi, Z., Nørgaard, K., Kjølstad, P.N., Madsen, H., and Jørgensen, J.B. (2017). Fault and meal detection by redundant continuous glucose monitors and the unscented Kalman filter. *Biomedical Signal Processing and Control*, 38, 86–99.
- Monnier, L., Colette, C., Wojtusciszyn, A., Dejager, S., Renard, E., Molinari, N., and Owens, D.R. (2017). Toward defining the threshold between low and high glucose variability in diabetes. *Diabetes Care*, 40(7), 832–838.
- Phillip, M., Battelino, T., Atlas, E., Kordonouri, O., Bratina, N., Miller, S., Biester, T., Stefanija, M., Muller, I., Nimri, R., and Danne, T. (2013). Nocturnal glucose control with an artificial pancreas at a diabetes camp. *New England Journal of Medicine*, 368(9), 824–833.
- Pinsker, J.E., Lee, J.B., Dassau, E., Seborg, D.E., Bradley, P.K., Gondhalekar, R., Bevier, W.C., Huyett, L., Zisser, H.C., and Doyle, F.J. (2016). Randomized crossover comparison of personalized mpc and pid control algorithms for the artificial pancreas. *Diabetes Care*, 39(7), 1135–1142.
- Reddy, M., Herrero, P., Sharkawy, M., Pesl, P., Jugnee, N., Pavitt, D., Godsland, I., A, G., Toumazou, C., Johnston, D., Georgiou, P., and Oliver, N. (2016). Metabolic control with the bio-inspired artificial pancreas in adults with type 1 diabetes: A 24-hour randomized controlled crossover study. *Journal of Diabetes Science and Technology*, 10(2), 405–413.